CHABLIS – A MOBILITY BREADBOARD VEHICLE FOR THE ESA'S MARS SAMPLE FETCH ROVER

[1]*Ghotbi, B., [1]Verzijlenberg, B., [1]Philip, A., [1]Jessen, S., [1]Nayeer, N., & [1]Schmidt, M.
[1]MDA, 9445 Airport Road, Brampton, Ontario L6S 4J3, Canada
Bahareh.ghotbi@mda.space
*Corresponding author

Abstract

The development of the Sample Fetch Rover for the Mars Sample Return (MSR) campaign led by ESA and NASA necessitated the design and validation of a mobility concept through the development of a mobility breadboard. This paper introduces CHABLIS, a mobility breadboard developed by MDA, and summarizes the test campaign to validate the mobility concept to meet the requirements of the MSR.

1. Introduction

For the purpose of returning Martian rock and soil samples to Earth for scientific study, a collaboration between the European Space Agency (ESA) and the National Aeronautics and Space Administration (NASA) known as the Mars Sample Return (MSR) campaign was launched. This would allow the use of powerful terrestrial instruments, infeasible for in-situ use on Mars, for scientific study and in search for evidence of past life on Mars.

On February 18, 2021, the first part of the MSR campaign began with the successful arrival of the NASA Mars 2020 Perseverance rover at the Jezero Crater on Mars. One of the rover's tasks is to collect a geologically diverse set of samples of the Martian surface and store them in sealed tubes. These tubes are to be placed in a cache at a known location on the Martian surface for later retrieval. In the second phase of the MSR, a Sample Retrieval Lander (SRL), carrying the Sample Fetch Rover (SFR), will land close to the location of the sample tube cache (between 200m and 2km) and deploy the SFR to the surface, which will travel to the sample tube depot and collect up to 30 sample tubes. After traveling back to the SRL, the tubes will be transferred to a Mars Ascent Vehicle (MAS) which will be launched into Mars orbit. The third phase of the mission will involve launching the Earth Return Orbiter (ERO), which will journey to Martian orbit to capture the MAS payload containing the sample tubes. Finally, the ERO will return to Earth where the sample tubes will be landed on the Earth's surface to a facility where the samples will be removed for study. A summary of the different phases of the MSR campaign can be seen in Fig. 1.

The SFR is one of the ESA's critical contributions to the MSR campaign, since it will serve as the key interface

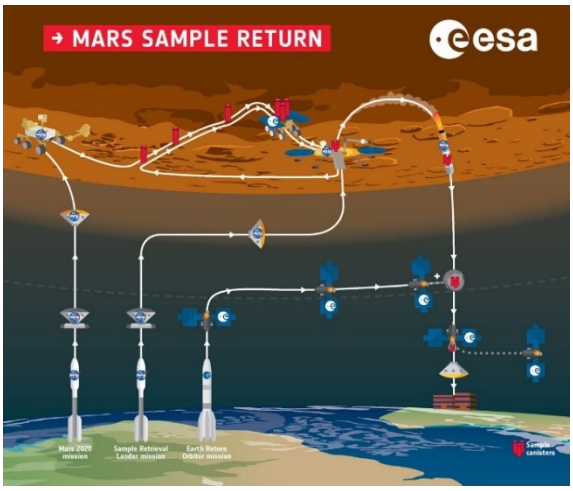

Figure 1: Overview Mars Sample Return campaign architecture (courtesy ESA – K. Oldenburg).

between the sample collection performed by the Perseverance rover and the launch of the samples into orbit through the MAS. The SFR is being built by Airbus UK for the ESA and its locomotion subsystem is developed by MDA Canada [1]. Previous Mars rovers are science platforms, with a traverse scenario that targets drives to surface features of scientific interest. SFR's main mission; however, is to retrieve and deliver previously obtained samples. To do so, SFR's daily activities are solely focused on traverse operations with SFR travelling faster over rougher terrain than previous rovers to achieve its objectives. The SFR mobility subsystem, Fetch Actuator System for Traverse (FAST), is a unique mobility architecture. This is coupled with use of a development a wheel-tire assembly provided by NASA. There were a number of key unknowns regarding the performance behaviour of this mobility system. The Characterisation Breadboard for Locomotion of Sample Fetch Rover (CHABLIS) mobility system was developed by MDA to understand the operational behaviour and to mitigate the impact of these unknowns on the overall SFR performance. Specifically, CHABLIS is used to de-risk the SFR locomotion design concept and quantify performance limits and loads of the SFR through various mobility tests representative of expected scenarios. In addition, the CHABLIS is used to evaluate the performance of NASA's next-generation flexible Mars wheel-tire assembly. In the sections to follow, the design of the CHABLIS will be examined, and then the test campaign conducted to validate the design and collect

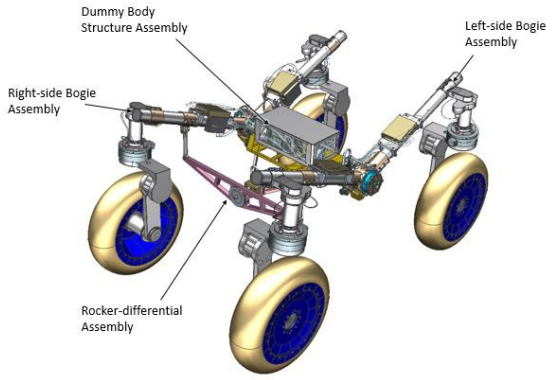

Figure 2: SFR CHABLIS BB Electro-Mechanical Assembly Component Identification

data for further improvements to the components of the FAST will be described, along with a discussion of the results from the tests.

2. Design

The CHABLIS represents key features of the flight SFR mobility system based on designs to date; it is kinematically equivalent and with a weight equivalent to its expected Martian weight in order to accurately assess the mobility performance of the design. The wheel-tire assemblies provided by NASA Glenn Research Center (GRC) are integrated with the rover breadboard for evaluation with the rest of the mobility subsystem. A suite of force and moment sensors is incorporated on the system and within the test facility to record the relevant data. The final CHABLIS design is shown in Fig. 2 and highlights key elements of structure.

CHABLIS was developed in accordance to the following high-level objectives: validating the locomotion concept of SFR, evaluating the mobility capability limits with an emphasis on obstacle negotiation performance, evaluating the wheel performance, and identifying areas of improvement on the SFR mobility design.

Given these objectives, CHABLIS design needs to be kinematically equivalent to the SFR mobility concept, inclusive of a four wheel, all-wheel drive and steering system along with a pitch averaging suspension; and a track width and wheelbase matching the flight architecture. In terms of maneuverability, it requires the ability to accept body-level velocity and angular rate commands to support generic Ackermann and generic point-turn manoeuvres and to accept individual actuator-level commands. Wheels need to be representative of the SFR fight wheel design from the perspective of size, traction performance, stiffness, and mass. The load distribution on the wheels should reflect the load distribution on the SFR flight wheels, such that the Centre of Gravity (CG) of the CHABLIS is similar to SFR and weight on wheels in Earth gravity is similar to that of the SFR wheels on Mars. Furthermore, actuator torque-speed capabilities and control system design for body-level and actuator-level control need to be representative of the flight SFR design. Finally, mobility characterization tests have to be done in a simulated Mars terrain environment with soil simulants and rocks representative of the expected terrain conditions for SFR.

The CHABLIS Breadboard consists of:

- A left side bogie assembly
- A right side bogie assembly
- A differential assembly
- Wheel-tire assemblies
- Control electronics, software, and harnessing
- Drive and steering actuators
- Force torque sensors
- A dummy body

CHABLIS operations can be controlled either through hand controller input or by means of a scripted sequence of commands. Hand controller or scripted test sequences to send body-level velocity commands to the Breadboard (BB) are converted into appropriate actuator-level commands by CHABLIS avionics depending on the mode of operation and the commanded manoeuvre. Scripts can also sequence independent actuator level commands in terms of angular velocity (drive) and position (steering) of the actuators.

The CHABLIS system provides the following modes of operation:

- Generic Ackermann Mode
- Generic Point Turn Mode
- Actuator Position Mode
- Actuator Velocity Mode

3. Test Campaign and Results

In order to identify the mobility limits of the breadboard design, gauge its performance, and characterize the interactions between the wheel-tire assembly and terrain, a test campaign was held. The CHABLIS test campaign took place over the course of five months in late 2021 and early 2022 at a test facility at RUAG [2]. This test facility was originally developed for a test program for the ExoMars rover and was modified to fit the testing requirements for the CHABLIS test campaign. The main test area contains a tilt table with a 6m by 6m test bed, which contains the soil samples and terrain used for the test, and which can be tilted to a maximum of 26 degrees. A crane is used to lift the rover into position for the tests. The facility was equipped with a VICON 3D motion tracking system to visually track and capture the 3D pose of the rover at 100Hz using a set of 8 cameras located around the test area, as well as several video cameras providing different view angles of the test bed. In addition, a separate test bed was available for single-

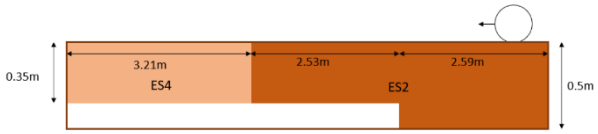

Figure 3: Single wheel test bed configuration

wheel tests, of which further details can be found in Section 3.1.

A significant part of the campaign was devoted to slope and obstacle climbing tests which can help predict the traverse ability of the SFR to inform the Guidance, Navigation and Control (GN&C) subsystem. The outcome of these tests together with other mobility tests such as steering, crevasse negotiation, and blocked load will be used to assess the actuator requirements, traction performance of the wheels, and generally the loads experienced by the rover. A subset of tests also included mobility across obstacles arranged to represent the expected nominal and worst case terrain roughness to better inform the design and help with improved estimates for energy consumed during traverse. Furthermore, the system energy budget and timeline which have previously been estimated using mathematical models can be enhanced using the actuator power and wheel slip data from test results.

3.1. Single-Wheel Tests

In order to determine the influence of depth of soil on the performance of the rover, as well as characterize the wheel-soil interaction, a set of tests using RUAG's single-wheel testbed [3] were carried out. These involved testing on 0.35m and 0.5m depth of ES2 soil, and 0.35m depth of ES4, as seen in Fig. 3. Initially, a 0.55m value of high soil depth was selected to assess the performance when the soil depth is equal or greater than the wheel diameter, however due to a limitation of the testbed maximum depth, a 0.5m value was chosen. A 0.35m value of low soil depth was chosen due to that being the maximum depth for ES4 soil able to be accommodated by the test bed. The wheel-soil interaction results would help inform simulation analysis.

As can be seen on Fig. 4, there seemed to be no variation that could be attributed to the soil depth under 120N wheel load. Due to facility limitations, the 225N wheel load test case could only be performed up to 50% slip ratio, but the results showed that no trend was visible and a linear relationship between the load and drawbar pull is considered suitable to estimate wheel performance under nominal load. In Fig. 4, it can be seen that a high drawbar pull is exerted for both ES2 and ES4 at 20% slip, after which it remains relatively constant up to around 60%, after which it starts increasing again. This suggests that in cases where additional force is required, such as climbing an obstacle or a high slope, the slip ratio would quickly grow from less than 20% to 80% or more.

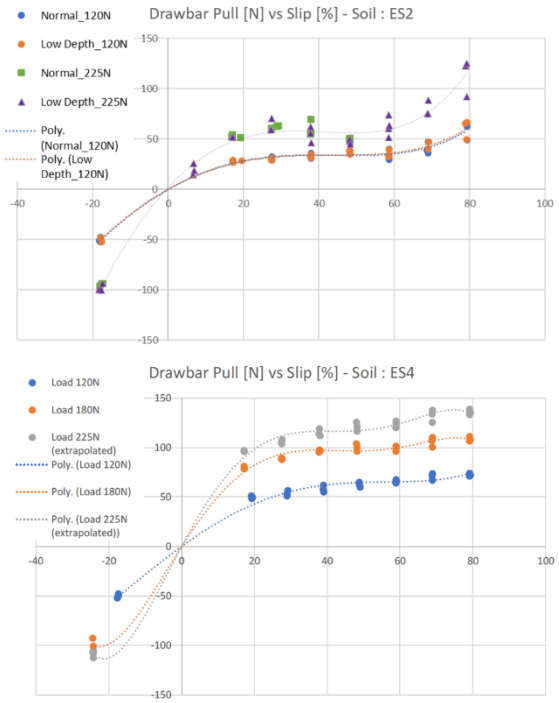

Figure 4: Drawbar pull vs. Slip on ES2 and ES4

Table 1: Steering test results

Steering mode	Slope	STR Current (A) (max)	STR Torque (Nm) (max)
S path	0	0.84	46
S path	10	0.86	47
Point turn	0	0.81	44
Point turn	10	0.82	45

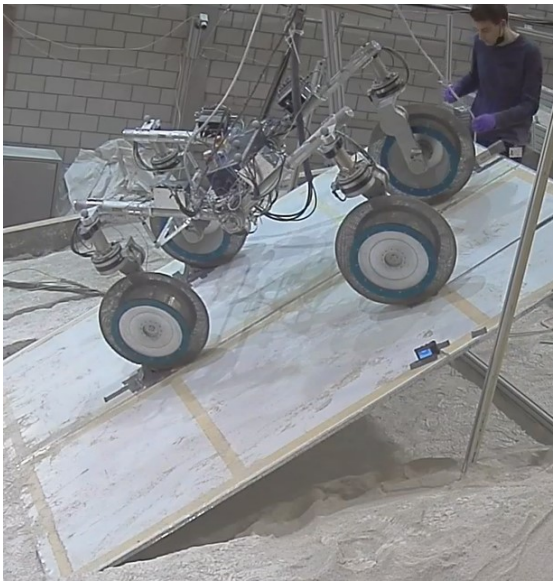

Figure 5: Stability test

Table 2: Slope negotiation test results

Slope (°)	Slip (%)			Normal forces (N) (min, max)			Drive torque (Nm) (min,max)			Traction (N) (min, max)		Friction Coeff. (-) (min,max)
	ES2	ES4	BED	ES2	ES4	BED	ES2	ES4	BED	ES2	ES4	BED
0	3	2	-6	238, 203	197, 244	212, 233	23, 33	18, 24	13, 21	83, 120	77, 57	0.17, 0.29
4	5	-	-	249, 190	-	-	24, 32	-	-	87, 116	-	-
8	9	-	-	181, 258	-	-	24, 35	-	-	87, 127	-	-
10	-	5	-10	-	199, 260	176, 261	-	25, 33	21, 33	-	83, 110	0.27, 0.42
12	29	-	-	155, 284	-	-	31, 51	-	-	113, 185	-	-
15	-	9	2	-	155, 273	151, 287	-	28, 40	28, 41	-	96, 135	0.38, 0.48
20	-	16	11	-	139, 281	140, 284	-	31, 53	28, 41	-	107, 182	0.39, 0.48
25	-	26	10	-	123, 288	113, 291	-	30, 66	34, 52	-	104, 229	0.63, 1.05

Table 3: Cross-slope negotiation test results

Cross slope (°)	Longitudinal slip (%)			Lateral slip (%)			Delta heading angle (deg)		
	ES2	ES4	BED	ES2	ES4	BED	ES2	ES4	BED
8	0.05	-	-	3.02	-	-	1.73	-	-
10	-	0.06	-	-	3.51	-	-	2.01	-
12	0.22	-	-	6.68	-	-	3.82	-	-
15	-	-	0.12	-	-	4.81	-	-	2.75
16	1.01	0.12		14.23	4.84	-	8.10	2.77	-
20	-	0.41	0.44	-	9.11	9.39	-	5.20	5.36
25	-	1.50	1.38	-	17.36	16.66	-	9.85	9.46

3.2. Stability and Steering

The static stability of the rover was tested by positioning it in 3 different orientations (longitudinal, lateral, and diagonal to the direction of the slope) on the slope, and then raising the slope, as seen on Fig. 5. The rover was observed to remain stable for an angle up to 36 degrees for the longitudinal and diagonal case, and 35.8 degrees for the lateral case. In addition, the ability of the rover to perform a point turn and s-path was tested on ES2 terrain to assess the torque required for the trajectories. In all cases, the trajectory was performed successfully within the error margin with the maximum steering current and torque as listed in Tab. 1.

3.3. Slope and Cross-Slope Performance

The ability of the rover to ascend a slope in bedrock, ES4, and ES2 terrain was assessed with various slope angles, as can be seen in Fig. 6. The results can be seen in Tab. 2, with the slip ratio, range of normal forces and generated torques on the wheels, as well as the traction (on ES2 and ES4 soil) and calculated friction coefficient (on bedrock). The friction coefficient was calculated as follows:

$$T_{rr} = F_n * C_{rr} * r$$
$$F_t = (T - T_{rr}) / r$$
$$Mu = F_t / F_n$$

where T_{rr} is the tire rolling resistance torque, F_n the normal load on the wheel, F_t is the traction force developed at the wheel-bedrock interface, C_{rr} the coefficient of rolling resistance (provided by NASA/GRC from tests), and r the wheel radius.

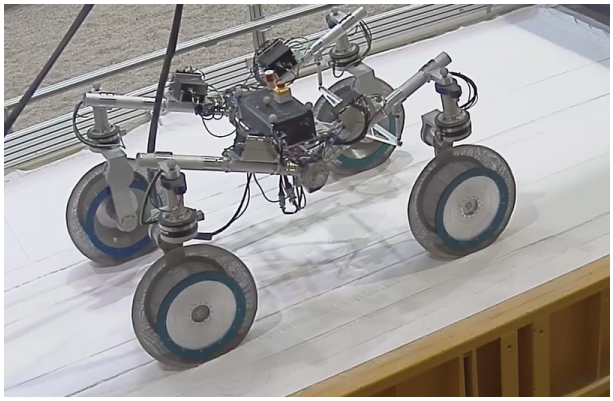

Figure 6: Slope negotiation test (on ES2 soil)

Table 4: Obstacle max height test results

Slope (°)	Obstacle height			Max drive torque (Nm)			Max slip (%)			Max impact force (N)
	ES2	ES4	BED	ES2	ES4	BED	ES2	ES4	BED	BED
0	32.5	32.5	31.0	152	120	115	88	74	32	214
4	29.5	-	-	122	-	-	82	-	-	-
5	-	29.5	-	-	120	-	-	75	-	-
8	29.5	-	-	142	-	-	82	-	-	-
10	-	25.0	31.0	-	116	156	-	75	83	370
12	25.0	-	-	153	-	-	93	-	-	-
15	-	18.0	27.0	-	109	15	-	71	73	287
20	-	10.0	15.0	-	93	20	-	64	74	243

In theory, the average friction coefficient has to the tangent of the slope angle. However, in this series of tests higher friction coefficient values were obtained. This can be due the following uncertainties:

- The calculated drive torque based on the logged current is higher than the real output torque of the actuators. This discrepancy can be the result of inaccuracy in actuator characterization in which the losses are estimated less than reality.
- The tire rolling resistance in higher than assumption used in the calculations. This is unlikely because the effect of C_{rr} is not significant.

The existing uncertainties can lead to an overestimation of friction coefficient. However, the objective of this test was mainly the assessment of climbing capability and the required actuator torque to support the climb. The torque values (in all the tables) therefore were accepted as conservative inputs for actuator design, even though they can be assumed to be larger than reality.

On bedrock and ES4 soil, a smooth manoeuvre was observed for slopes up to a maximum of 25 degrees, with relatively low slip ratios. For ES2 soil, low sinkage was observed up to an 8 degree slope, after which the sinkage grew significantly until it impeded steady-state motion at 16 degrees. The sinkage increased with increasing slip, to where the required traction to overcome resistance causes even more slippage.

Tests were also carried out to assess the ability of the rover to negotiate a cross-slope. The maximum slopes identified in the previous tests (25 degrees on bedrock and ES4, and 16 degrees on ES2) were also taken as the maximum slopes to be used for these tests, and the longitudinal and lateral slip, and the change in the heading angle were calculated for each slope and terrain type, as seen in Tab. 3. While longitudinal slip remained low throughout, lateral slip saw an increase at higher slopes (above 12 degrees for ES2 and above 20 degrees for ES4 and bedrock) analogous to the slope ascending performance in the previous test set.

Figure 7: Obstacle negotiation test

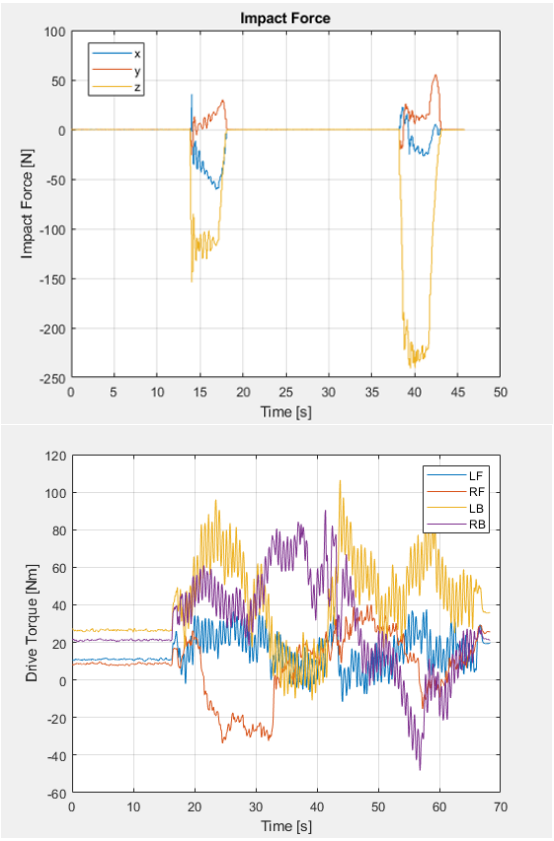

Figure 8: Impact force and drive torque for an obstacle negotiation test

Table 5: Obstacle negotiation test results

Obstacle height	Slope (°)		Max drive torque (Nm)			Max slip (%)			Max impact force (N)
	ES2	ES4/BED	ES2	ES4	BED	ES2	ES4	BED	BED
5.0	-	20	-	79	-	-	67	-	-
9.0	-12	-20	37	18	29	31,-83 (skid)*	20, -200 (skid)*	28, -136 (skid)*	426
	0	0	61	60	63	21	22	23	221
	4	10	67	74	74	25	31	74	230
	8	15	72	70	77	32	47	77	244
	12	20	113	-	85	72	-	64	253
13.0	-	20	-	-	105	-	-	63	240
16.0	-	15	102	-	-	85	-	-	-
18.0	-12	-20	53	41	54	35, -129 (skid)*	40, -358 (skid)*	57, -229 (skid)*	348
	0	0	83	81	75	44	50	42	309
	4	10	93	103	93	62	51	54	253
	8	15	106	-	103	66	-	59	211
	12	20	116	-	-	84	-	-	-
22.0	-	10	93	-	-	61	-	-	-
23.0	-	-20	-	-	50	-	-	59,-243 (skid)*	381
25.0	-	15	-	-	143	-	-	85	316
27.5	-12	-20	83	69	-	55,-190 (skid)*	40, -218 (skid)*	-	-
	0	0	108	99	105	85	57	65	394
	-	10	-	-	143	-	-	68	309

3.4. Obstacle Negotiation

The first test objective for assessing obstacle negotiation was to establish the most difficult shape of obstacles for the rover, and so a set of tests was conducted with rectangular, hemispherical, and pyramidal obstacles, all of a 15 cm height and on a 12 degree slope. The pyramidal shape was the least difficult, with 99 Nm of max torque produced and 69% max slip, followed by hemispherical, with 108 Nm max torque and 67% max slip. The most difficult shape was rectangular, with 111 Nm of torque and 74% max slip, and hence became the shape of obstacle chosen for the rest of the obstacle negotiation tests.

The next set of tests were aimed at identifying a maximum obstacle height for each terrain type and slope angle, which could then be used as an upper bound to test obstacle negotiation. An example of the test setup can be seen in Fig. 7,Figure 7 and the results can be seen on Tab. 4. Obstacles with heights 25.0-32.5cm were identified as climbable on ES2 up to 12 degrees slope, while for bedrock it ranged 15.0-31.0 cm and 10.0-32.5 cm for ES4 up to 20 degrees slope. In all cases, attempts to climb larger obstacles failed during the rear wheel climb phase.

Finally, a test matrix was created to test the obstacle negotiation of the rover for each terrain type, bounded by maximum obstacle heights and slopes (uphill and downhill) identified in the previous test sets. This resulted in the data provided on Tab. 5, showing the maximum drive torque, slip ratio, and impact force in each terrain type, obstacle height, and slope angle combination. For bedrock test cases, the impact force was measured using a force-impact plate placed at the foot of the obstacle where the descending wheel of the rover would land. The impact data acquired was plotted, such as for the 13.0cm obstacle case in Fig. 8 (z-axis normal to the impact plate, x-axis in the longitudinal direction), which also includes a plot of the drive torque on each wheel during the traversal (wheels labelled as Left Front, Right Front, Left Back, and Right Back in the plot). For ES2 soil, the manoeuvre was smooth with some sinkage developed to support the climb, a significant amount of which was developed to cross the largest obstacle tested on flat terrain (27.5cm) and 12 degrees slope (18.0 cm). The downhill cases were also smooth but had some skidding on the descent from the obstacle. Likewise in the ES4 and bedrock tests, smaller obstacle height and lower slope combinations were fairly smooth, with small heading changes due to slip with increasing obstacle height and slope. A considerable heading change occurred in one of the most difficult bedrock test cases, with a 25.0 cm obstacle on a 15 degree slope. On the other hand, the downhill cases for ES4 and bedrock saw an easy climb but significant skidding while driving off the obstacle.

A small set of tests were also done to monitor the deformation of the wheels over a crevasse on flat, 10, and 20 degree slopes, an example of which can be seen on

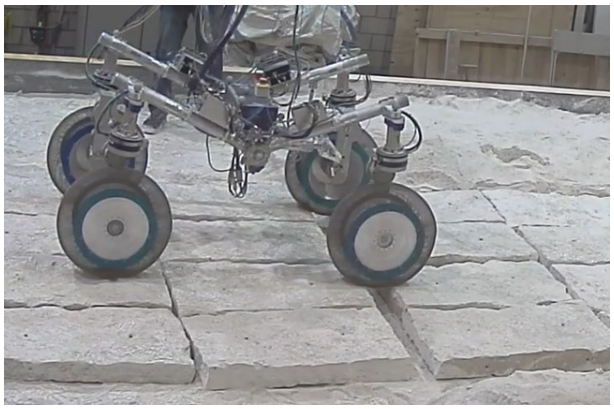

Figure 9: Crevasse traversal test

Figure 10: Wheel deformation during crevasse test

Fig. 9. As seen on Fig. 10, no significant wheel deformation could be seen.

In addition, a set of tests were done to measure the max drive and steering torques during a blocked load scenario, as seen on Fig. 11. To avoid the wheel trying to climb the obstacle due to a constant command speed, a joystick was used to control the command speed. Both blocked load configurations resulted in the right front wheel stopped by the two obstacles as it was commanded to drive forwards and steer, the results of which can be seen on Tab. 6.

Table 6: Blocked load test results

Slope (°)	Config. (Figure)	Max Normal Load (N)	Max Radial Load (N)	Max drive torque (Nm)	Max steer torque (Nm)
0	A	322	273	114	49
0	B	343	290	132	49

3.5. Terrain Traversal

From past experience of performing life tests for the Mars 2020 rover wheels, NASA/JPL developed a set of tests to characterize the loads on the wheel-tire assembly and interaction of the rover with rocky terrain that it would be expected to encounter. The results would help inform the design of single-wheel life tests and provide

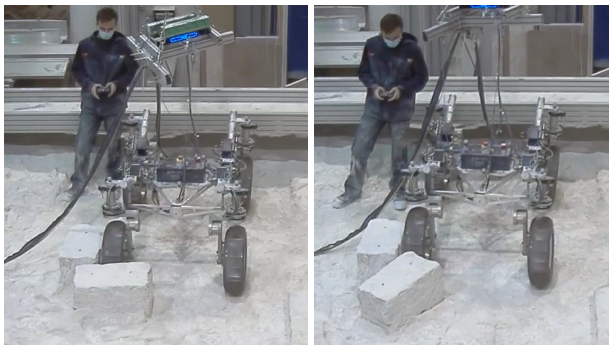

Figure 11: Blocked load test, configuration A (left) and B (right)

Figure 12: Terrain traversal test, Life Terrain (top) and 10% CFA (bottom)

an update for the power and energy budget for the rover while it is traversing the types of rocky terrain as featured in these tests. Tiles of 3 different terrain types were prepared by NASA/JPL: Life Terrain based on Mars 2020 terrain used in previous wheel life tests, and 5% Cumulative Fractional Area (CFA) and 10% CFA terrain based on orbital imagery of the proposed landing site. For each of these terrain types on a flat slope, and increasing slope angles for the CFA terrains, the rover was made to traverse the terrain tiles in both directions, examples of which can be seen in Fig. 12. The resultant torques and forces on the wheels were measured, as well as the slip ratios, power, and energy density during the traverse.

For all the test cases on a flat slope, the rover was able to successfully cross the tiles, with very low slip. The energy density varied from 245-383 J/m, with 5% CFA resulting in the lower values, 10% CFA in the middle, and the Life Terrain resulting in the higher values. The range of slopes used for the sloped test cases targeted a 12 degree slope for 10% CFA and 20 degrees for 5% CFA, with additional slopes in the 12-25 degree range being tested as well. In these sloped test cases, the power

Table 7: Terrain traversal test summary

Terrain type	Slope (°)	Direction	Energy Density (J/m)
Life Terrain	0	-	383.48
10% CFA	0	-	301.91
5% CFA	0	-	245.36
10% CFA	12	Down	183.68
10% CFA	12	Up	542.16
5% CFA	20	Down	74.05
5% CFA	20	Up	400.27

and energy density were highest for 10% CFA in the uphill direction and lowest for 5% CFA in the downhill direction, a summary of which can be seen in Tab. 7 for the target test cases. The rover was able to cross the tiles successfully in the sloped test cases, however there was significant difficulty in climbing the larger rocks on the highest slope used for each terrain (18 degrees for 10% CFA and 25 degrees on 5% CFA) while going uphill, causing the wheel to slide off while climbing or cause a heading change to bypass the rock entirely. Slight changes in the heading were also seen in the downhill cases where some skidding took place as the wheels descended off the larger rocks.

4. Conclusions and Future Work

The CHABLIS test campaign was a very successful risk-mitigation activity that tackled the most significant uncertainties for SFR/FAST mobility. It validated the vehicle concept that allows for near-direct use of CHABLIS concepts for path-to-flight FAST that will be implemented for FAST LVM (Locomotion Verification Model) & STM (Structural & Thermal Model) prior to detailed flight FAST development. This campaign addressed all the high-priority items in the test plan and completed a selection of the low-priority ones while staying on schedule.

CHABLIS test results will be used to calibrate a simulation tool that will enable rapid assessment of off-nominal scenarios for varying vehicle configurations (i.e. mass, form-factor for wheel-base/track-width/centre of mass). The simulation tool can assess impact to subsystem requirements (wheel-tire assembly, actuator, bogie) for torque, mobility loads, and other specific variables. The outcome of the CHABLIS test campaign will be used to validate the mobility envelope in terms of soil type, slope, obstacle negotiation, and obstacle shape, to name a few, and to support mission planning and sizing of non-FAST systems. The single-wheel test results will help improve the wheel-soil interaction models that are critical for predicting the rover behaviour on the Martian surface. The validated mobility capability limits will inform GN&C on the type of terrain features that have to be avoided. Based on the test data, the mobility performance for a range of scenarios in terms of required actuator torque and power was evaluated. The energy and time penalty associated with a selection of slope, terrain type, and obstacle sizes were calculated, which will help GN&C optimize path planning. The force/torque measurements from the on-board force/torque sensors and impact plates will inform the structural analysis of the SFR and design of components such as actuators and the wheel-tire assembly.

This campaign was a very successful rehearsal for the future FAST LVM test campaign. The lessons learnt include improvements to rover integration with the test facility, data acquisition and transfer, actuator characterization, test plan and schedule, rover development, and sensor selection and placement.

Acknowledgements

We would like to thank ESA, NASA/JPL, NASA/GRC, and RUAG, without whom this work would not have been possible.

References

1. Ridolfi, P., Pecover, D., Pulker S., Wayman, A., Zekri, E., Zwick, M., Do, S., Eremenko, A., Heverly, M., Moreland, S., Nicholas, A., Asnani, V., Ghotbi, B., Jessen, S., Rehmatullah, F. (2021). Development of the Sample Fetch Rover Locomotion Subsystem. In Proc. 72nd International Astronautical Congress, Dubai, United Arab Emirates.

2. Michaud, S., Von Rohr, S., Oettershagen, P., Halter, B., Grégoire, F., Poulakis, P. (2022). Developing and Using a Facility Enabling Characterization and Qualification of Planetary Exploration Rover Mobility. In Proc. 16th Symposium on Advanced Space Technologies in Robotics and Automation.

3. Oettershagen, P., Lew, T., Tardy, A., Michaud, S. (2019). Investigation of Specific Wheel-Terrain Interaction Aspects Using an Advanced Single Wheel Test Facility. In Proc. 15th Symposium on Advanced Space Technologies in Robotics and Automation.